

Particle Correlations in Jets

Wenbin Zhao,^{1,2,*} Volker Koch,^{1,†} and Feng Yuan^{1,‡}

¹*Nuclear Science Division, Lawrence Berkeley National Laboratory, Berkeley, CA 94720, USA*

²*Physics Department, University of California, Berkeley, California 94720, USA*

We study particle correlations in high energy jets by comparing the measured energy-energy correlator (EEC) with that constructed from two individual energy flows with respect to the jet axis. This comparison demonstrates that genuine correlations exist for small angle and moderate/large angle, indicating that they are coming from correlated splitting. This method will provide a unique tool to disentangle different physics, by comparing the genuine correlations in jet EEC between heavy ion collisions and proton-proton collisions. It will help to expose the medium modification of parton splitting in hot QCD medium. On the other hand, the medium responses are expected to be canceled out in the genuine correlations.

Introduction. Energy-energy correlators (EECs) in e^+e^- annihilation were introduced to test the asymptotic freedom of QCD more than three decades ago [1–3]. Theoretical developments have advanced its physics as one of the important places to study precision strong interaction physics [4–15]. In recent years, a renaissance of interest of EEC has spanned across different fields [16–54], see, a recent review [55]. In particular, it has been extensively applied to systematic measurements of jet substructure in proton-proton collisions and heavy ion collisions at the LHC and RHIC [56–61]. In the following, we study this physics from a different perspective, focusing on the correlation between particles inside the high energy jets. The goal is to help us to understand the underlying physics and to reveal hadronization effects in these correlation measurements.

The EECs inside the jet is defined as

$$\begin{aligned} & \frac{d\langle \text{EEC}(\theta) \rangle_{\text{full}}}{d^2\theta} \\ &= \frac{1}{N_{jet}} \sum_{jets} \sum_{i \neq j \in J} \frac{E_i E_j}{E_J^2} \delta^{(2)}(\vec{\theta} - (\vec{\theta}_i - \vec{\theta}_j)), \end{aligned} \quad (1)$$

where N_{jet} represents number of jets. The sum is over all particles (i, j) in the jet so that $\text{EEC}(\theta)$ corresponds to the energy weighted sum (distribution) of all pairs with relative angle θ , and jet energy $E_J = \sum_i E_i$. At colliders, the definition of the angle includes the rapidity difference between the two particles, e.g., $R_L = \sqrt{\delta\eta^2 + \delta\phi^2}$ is used in pp collisions where $\delta\eta$ represents the rapidity difference and $\delta\phi$ for the azimuthal angle difference. However for small angle $R_L = \theta$ to very good approximation. In the transverse plane perpendicular to the jet axis, each angle represents the distance between the particle and the jet axis. Because they are all within the jet with a small jet size, the angular distribution from the above will peak at small angle and the dominant contributions from perturbative QCD come from collinear radiation.

The soft gluon radiation is suppressed due to the energy weight. Therefore, a perturbative QCD prediction can be applied to the EEC observables [1].

In the perturbative collinear region ($\theta > 0.1$), additional gluon radiations to all orders can be resummed through a factorization approach [13] with logarithmic corrections. With additional contributions from renormalons [15] and power corrections [33, 34], these precision improvements play an important role to describe the experimental data from EECs in e^+e^- annihilation. Toward the other end in the angular distribution ($\theta \sim 0$), additional physics has to be taken into account such as the assumption of a “free hadron” phase [22]. Recently, a non-perturbative transverse momentum dependent (TMD) fragmentation mechanism has been proposed to describe the distribution in this region [40, 43] and further theoretical developments along this direction have been reported [49–54].

While the EEC, Eq. (1), is commonly called a “correlator” it is actually an energy weighted pair distribution, and thus will not vanish even in the absence of any particle correlations in the jets. To extract the true, genuine correlations one typically subtracts the product of the single particle distributions, which remove all uncorrelated pairs. Alternatively one uses mixed events to determine the uncorrelated pair distribution. In the context of hadronic physics this is for example done for particle interferometry measurements to determine the size of the particle emitting source [62]. In this paper we will take exactly this approach in order to extract and identify the true two-particle correlations.

Performing such an analysis will enable us to highlight the physics behind the three different regions in the EEC in jet. In particular, we find that the correlation is significant in both small and moderate θ regions. Although their physics are totally different – non-perturbative TMD fragmentation dominates small θ while collinear splitting dominates the moderate $\theta > 0.1$ – they both come from correlations, i.e., two particles originating from one source. In this study, we employ the PYTHIA8.306 event generator [63] to demonstrate our proposed approach.

Trivial two particle distributions from single

* WenbinZhao@lbl.gov

† vkoch@lbl.gov

‡ fyuan@lbl.gov

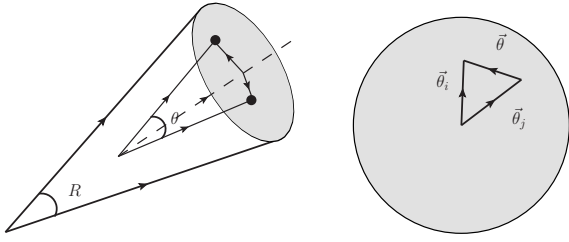


FIG. 1. Energy-Energy Correlator measurement inside the jet. The two particles are at relative angles respect to the jet axis: $\vec{\theta}_i$ and $\vec{\theta}_j$. Their angular difference $\vec{\theta}$ is defined as a 2-dimension difference in the plane perpendicular to the jet axis.

particle distributions. The trivial two particle distributions based on the single particle distributions need to be carefully defined. For this purpose, the jet axis can be used as an appropriate reference. As shown in Fig. 1, in the experimental measurements, the energy correlations are counted against the particles inside a jet. Therefore, a jet axis can be identified. Because of the rotation symmetry around the jet axis, the above angular correlation is a two-dimensional distribution,

$$\vec{\theta} = \vec{\theta}_i - \vec{\theta}_j, \quad (2)$$

where $\vec{\theta}_i = \vec{P}_{i\perp}^h / (z_i E_J)$ represents the angle of hadron i with respect to the jet axis, and z_i is its momentum fraction of the jet energy. We consider a jet radius of $R \ll 1$. Therefore, $|\vec{P}_{i\perp}^h| \ll E_i = z_i E_J$, i.e., the transverse momentum of the hadron $|\vec{P}_{i\perp}^h|$ is much smaller than its longitudinal momentum E_i .

With the jet axis well defined, one can also define the correlator depending on two angles,

$$\frac{d\langle \text{EEC}(\theta_1, \theta_2) \rangle}{d^2\theta_1 d^2\theta_2} = \frac{1}{N_{jet}} \sum_{jets J} \sum_{i \neq j \in J} \frac{E_i E_j}{E_J^2} \times \delta^{(2)}(\theta_1 - \theta_i) \delta^{(2)}(\theta_2 - \theta_j), \quad (3)$$

from which we can derive the angular distribution of EEC of Eq. (1) [3],

$$\frac{d\langle \text{EEC}(\theta) \rangle}{d^2\theta} = \int d^2\theta_1 d^2\theta_2 \frac{d\langle \text{EEC}(\theta_1, \theta_2) \rangle}{d^2\theta_1 d^2\theta_2} \delta^{(2)}(\vec{\theta} - (\vec{\theta}_1 - \vec{\theta}_2)). \quad (4)$$

However, Eq. (3) contains un-correlated contribution from two energy flows through a trivial construction

$$\frac{d\langle \text{EEC}(\theta_1, \theta_2) \rangle}{d^2\theta_1 d^2\theta_2} \Big|_{\text{trivial}} \propto \frac{d\langle \text{E}(\theta_1) \rangle}{d^2\theta_1} \times \frac{d\langle \text{E}(\theta_2) \rangle}{d^2\theta_2}, \quad (5)$$

where the single energy distribution is defined as,

$$\frac{d\langle \text{E}(\theta) \rangle}{d^2\theta} = \frac{1}{N_{jet}} \sum_{jets J} \sum_{i \in J} \frac{E_i}{E_J} \delta^{(2)}(\vec{\theta} - \vec{\theta}_i). \quad (6)$$

The above equations will be used to construct the subtraction term for the genuine correlations.

To construct the trivial correlator, one has to properly take into account the energy weighting and, related to that, the normalization of the angular integral, of Eq. (1). Clearly, the latter is not normalized to 1. To account for this difference, we introduce a normalization factor for the trivial correlation

$$\frac{d}{d^2\theta} \langle \text{EEC}(\theta) \rangle_{\text{trivial}} = N_{\text{trivial}} \int d^2\theta_1 d^2\theta_2 \times \frac{d\langle \text{E}(\theta_1) \rangle}{d^2\theta_1} \frac{d\langle \text{E}(\theta_2) \rangle}{d^2\theta_2} \delta^{(2)}(\vec{\theta} - (\vec{\theta}_1 - \vec{\theta}_2)), \quad (7)$$

which has the same normalization as Eq. (1). For the typical jet energy at the LHC, we find that $N_{\text{trivial}} \approx 0.85$, which is also equal to the integral of Eq. (1) over θ for a particular jet energy range.

In experiment, one can also construct the above trivial correlation by means of mixing event or rather jet mixing. As detailed in Appendix A, one generates “mixed” jets by picking particles from random jets. For example, given a *true* jet with n particles the corresponding *mixed* jet is made with n particles with one each from n randomly selected true jets. Given the mixed jets, the trivial, un-correlated EEC correlator is then obtained from Eq. (1) where the true jets are replaced by the mixed jets with an additional normalization factor,

$$\frac{d\langle \text{EEC}(\theta) \rangle_{\text{mix}}}{d^2\theta} = C_{mix} \frac{1}{N_{jet}} \sum_{\text{mixed jets } J} \times \sum_{i \neq j \in J} \frac{E_i}{E_{J,i}} \times \frac{E_j}{E_{J,j}} \delta^{(2)}(\vec{\theta} - (\vec{\theta}_i - \vec{\theta}_j)). \quad (8)$$

To account for the proper summation of mixed jets at different rapidities, here we keep the original energy fraction for each particle, e.g., $E_i/E_{J,i}$ for particle i from Jet $_j$.

In the above equation, we introduce a normalization factor C_{mix} to account for the differences between the mixing jet events and the true jet events. The reason behind this is that the above sum favors particles with larger momentum fractions in the mixed jet, although the angular distribution remains. We have verified that the above two equations (7) and (8) lead to the same shape of the angular distribution of the trivial EEC for the jet production at the LHC (see Fig. 5 in the Appendix).

Similarly we can evaluate the single energy flow result from Eq. (6) by using mixed jets. As we show in the Appendix they agree with those obtained from the true jets, as they should.

Meanwhile, it has been shown in the literature that the particle distributions inside a jet can be described by the parton fragmentation functions in both the collinear case [64–66] and the TMD case [67–69]. In particular, a recent paper [70] has shown that the TMD fragmentation functions can be applied to the angular distribution of Eq. (6) with a typical parameterization [71]. In the Appendix, we show that these TMD fragmentation functions can also give a reasonable description of the trivial EEC at small angle.

Two Particle Correlations in a Jet. With these results, we now compare the correlations between Eq. (1) and (7). As we see from Fig. 2, they have a similar shape, peaked at small angles, but there are obvious differences which are due to the actual true correlations.

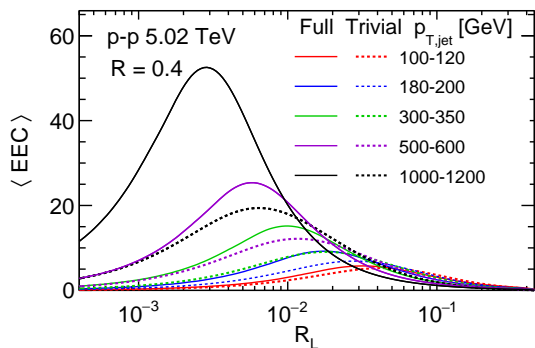


FIG. 2. The PYTHIA simulations of angular distributions for the EECs in jet for different jet energies at the LHC. Here, we compare the full correlation, $\langle \text{EEC} \rangle_{\text{full}}$, corresponding to the experiment measurements of Eq. (1) and the trivial correlation, $\langle \text{EEC} \rangle_{\text{trivial}}$, constructed from two separate energy flows of Eq. (7). Here, $R_L = \theta$ in these equations.

These genuine correlations can be extracted by the difference between the two correlators,

$$\langle \text{EEC}(\theta) \rangle_C = \frac{d\langle \text{EEC}(\theta) \rangle_{\text{full}}}{d^2\theta} - \frac{d\langle \text{EEC}(\theta) \rangle_{\text{trivial}}}{d^2\theta} \quad (9)$$

Again, the second term in the right hand side of the above equation can be obtained by the integral form of Eq. (7) or via mixed jets c.f. Eq. (8). The angular integral of the above correlation vanishes by construction. In Fig. 3 (upper plot), we show the above correlations, Eq. (9) as functions of $R_L = \theta$ for the typical jet energies at the LHC. It shows a characteristic behavior in different angular regions. In particular, in the large θ region toward the jet boundary, the correlation $\langle \text{EEC}(\theta) \rangle_C$ decreases with θ . This is because both terms in Eq. (9) vanish and their difference vanishes too. To expose a possibly interesting correlation signal in this region, it is advantageous to look at the the ratio of the two distributions,

$$\mathcal{R}_{\text{EEC}}(\theta) = \frac{d\langle \text{EEC}(\theta) \rangle_{\text{full}}}{d^2\theta} / \frac{d\langle \text{EEC}(\theta) \rangle_{\text{trivial}}}{d^2\theta}, \quad (10)$$

where the numerator and denominator come from Eq. (1) and (7), respectively. As shown in Fig. 3 (lower plot), this ratio demonstrates the strength of the correlation at both small and large angle of θ .

Experimentally, all of the quantities that define the correlations in Eqs. (9,10) can be measured. Therefore, these correlations can be systematically studied in experiments at the LHC and RHIC. There are a number of interesting observations from Fig. 3:

- Stronger correlations at both small and moderate angles for all jet energies. In addition, higher jet energies tend to have larger ratios in these two regions as well.

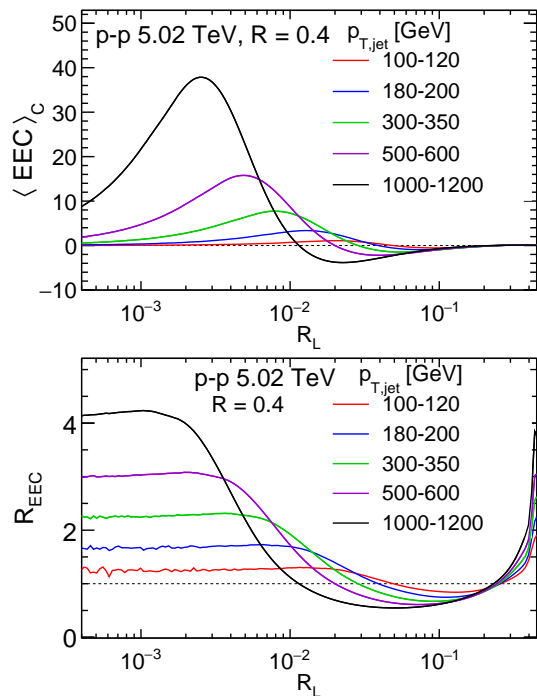


FIG. 3. The two particle genuine correlations in jets as functions of the angle between them for different jet energies at the LHC: (upper) defined as difference, Eq. (9) and (lower) defined as ratio, Eq. (10). Here, as above, $R_L = \theta$.

- Between these two regions, the lower the jet energies, the ratios are closer to 1. This means that the experiment measured EECs of Eq. (1) is close to the trivial EECs constructed from the individual energy flows Eq. (7).
- Three characteristic regions in this plot are very similar to those classified in Ref. [22], from “free hadrons” to “transition” to “collinear” regions, respectively. This demonstrates that the above ratio provides an alternative method to study the associated physics.

The ratio clearly highlights different physics in different kinematic regions. Experimental measurements of these genuine correlations will provide crucial information on the QCD dynamics involved in the particle correlations in high-energy jets and help to investigate hadronization effects at colliders energies. Especially, when the two hadrons are close to each other, they tend to be produced from a single non-perturbative fragmentation as suggested in Refs. [40, 43, 49–51]. The results shown in Fig. 3 expose these effects very clearly.

The correlation measurement proposed above will be also very useful in deciphering the underlying mechanism for the nuclear modification for the EEC observables, because it cancels out the single-particle nuclear effects inside the jet. For example, we can construct the difference/modification between the correlations of Eq. (9) for

AA and pp collisions,

$$\Delta\langle\text{EEC}\rangle^{AA}(\theta) = \langle\text{EEC}(\theta)\rangle_C^{AA} - \langle\text{EEC}(\theta)\rangle_C^{pp}, \quad (11)$$

or a double ratio,

$$\mathcal{R}_{\text{EEC}}^{AA}(\theta) = \frac{\frac{d\langle\text{EEC}(\theta)\rangle_{\text{full}}^{AA}}{d^2\theta} / \frac{d\langle\text{EEC}(\theta)\rangle_{\text{trivial}}^{AA}}{d^2\theta}}{\frac{d\langle\text{EEC}(\theta)\rangle_{\text{full}}^{pp}}{d^2\theta} / \frac{d\langle\text{EEC}(\theta)\rangle_{\text{trivial}}^{pp}}{d^2\theta}}. \quad (12)$$

We expect that the nuclear modification factors will be more evident in the regions of small and large θ where genuine correlations are expected to dominate.

For example, at very small angles, the dominant contribution comes from the jet energy loss. By studying the above double ratio, we may be able to directly extract the fraction of the jet energy loss in these measurements. This is because the correlation ratio is (almost) proportional to the jet energy (see bottom panel of Fig. 3). As a consequence, the ratio of Eq. (12) will be bigger than 1. The jet energy dependence of this double ratio shall provide crucial information on the jet energy loss as a function of the jet energy. Similarly, at large angle, we will be able to study the medium modification of the parton splitting. Again, the reason behind this is that in this region it is dominated by the splitting contributions.

In addition, it has been realized that the medium responses will modify the EEC of Eq. (1) in heavy ion collisions [30, 47], which might be mis-interpreted as the medium modification of parton splitting in the medium. However, by measuring the genuine correlations, the contribution from the medium response will be canceled out in Eqs. (9) and (10) in AA collisions, because the medium response has no particular angular dependence, see, for example, the discussions in Ref. [47]. That means there is no modification to Eqs. (11) and (12). This demonstrates that we can disentangle different physics in the measurements of the EEC in heavy-ion collisions by focusing on the genuine correlations.

We note that the above discussion applies to the EEC measurements in proton-nuclei collisions as well, where we can define similar correlations. From that, we can study the difference (or ratio) between the correlations

in pA collisions and those in pp collisions to investigate the underlying physics behind the nuclear modification observed in experiments [61].

Conclusion. In this paper, we have proposed to study the particle correlations inside high energy jets by constructing a trivial EEC through the two individual energy flows and comparing that with the measured EEC, as described by Eqs. (1) and (7). We have discussed the characteristic features of the ratios/differences defined from them as functions of angle between the two particles. The energy evolution of this ratio will help us to understand the underlying physics behind the energy-energy correlators and may reveal the hadronization effects in high energy jets at colliders.

We further propose to measure the double ratios of Eq. (12) between heavy ion collisions and proton-proton collisions as a crucial method to disentangle different contributions to the EEC observable. In particular, the near-side behavior of this double ratio will inform the jet energy loss fraction in heavy ion collisions and large angle double ratios will tell us about the medium modification of the parton splitting in the medium. On the other hand, we argue that the medium response will mostly be canceled out in these double ratios.

Our proposal could be straightforwardly extended to multi-point energy correlators. A comprehensive investigation of all of these correlators will deepen our understanding of QCD dynamics involved in these measurements.

ACKNOWLEDGMENTS

Acknowledgments This work is supported by the Office of Science of the U.S. Department of Energy under Contract No. DE-AC02-05CH11231. W.B.Z is also supported by the National Science Foundation under grant number ACI-2004571 within the framework of the XSCAPE project of the JETSCAPE collaboration and by the U.S. Department of Energy, Office of Science, Office of Nuclear Physics, within the framework of the Saturated Glue (SURGE) Topical Theory Collaboration.

-
- [1] C. L. Basham, L. S. Brown, S. D. Ellis, and S. T. Love, Phys. Rev. Lett. **41**, 1585 (1978).
 - [2] C. L. Basham, L. S. Brown, S. D. Ellis, and S. T. Love, Phys. Rev. D **17**, 2298 (1978).
 - [3] C. L. Basham, L. S. Brown, S. D. Ellis, and S. T. Love, Phys. Rev. D **19**, 2018 (1979).
 - [4] J. C. Collins and D. E. Soper, Nucl. Phys. B **193**, 381 (1981), [Erratum: Nucl.Phys.B 213, 545 (1983)].
 - [5] A. Ali and F. Barreiro, Phys. Lett. B **118**, 155 (1982).
 - [6] K. A. Clay and S. D. Ellis, Phys. Rev. Lett. **74**, 4392 (1995), hep-ph/9502223.
 - [7] D. de Florian and M. Grazzini, Nucl. Phys. B **704**, 387 (2005), hep-ph/0407241.
 - [8] V. Del Duca, C. Duhr, A. Kardos, G. Somogyi, and Z. Trócsányi, Phys. Rev. Lett. **117**, 152004 (2016), 1603.08927.
 - [9] Z. Tulipánt, A. Kardos, and G. Somogyi, Eur. Phys. J. C **77**, 749 (2017), 1708.04093.
 - [10] A. Kardos, S. Kluth, G. Somogyi, Z. Tulipánt, and A. Verbytskyi, Eur. Phys. J. C **78**, 498 (2018), 1804.09146.
 - [11] I. Moulton and H. X. Zhu, JHEP **08**, 160 (2018), 1801.02627.
 - [12] L. J. Dixon, M.-X. Luo, V. Shtabovenko, T.-Z. Yang, and H. X. Zhu, Phys. Rev. Lett. **120**, 102001 (2018), 1801.03219.

- [13] L. J. Dixon, I. Moulton, and H. X. Zhu, *Phys. Rev. D* **100**, 014009 (2019), 1905.01310.
- [14] M. A. Ebert, B. Mistlberger, and G. Vita, *JHEP* **08**, 022 (2021), 2012.07859.
- [15] S. T. Schindler, I. W. Stewart, and Z. Sun, *JHEP* **10**, 187 (2023), 2305.19311, [Erratum: *JHEP* **10**, 175 (2024)].
- [16] C. Lee and G. F. Sterman, *Phys. Rev. D* **75**, 014022 (2007), hep-ph/0611061.
- [17] C. F. Berger, T. Kucs, and G. F. Sterman, *Phys. Rev. D* **68**, 014012 (2003), hep-ph/0303051.
- [18] D. M. Hofman and J. Maldacena, *JHEP* **05**, 012 (2008), 0803.1467.
- [19] H. Chen, I. Moulton, X. Zhang, and H. X. Zhu, *Phys. Rev. D* **102**, 054012 (2020), 2004.11381.
- [20] K. Lee, B. Meçaj, and I. Moulton, *Phys. Rev. D* **111**, L011502 (2025), 2205.03414.
- [21] E. Craft, K. Lee, B. Meçaj, and I. Moulton, (2022), 2210.09311.
- [22] P. T. Komiske, I. Moulton, J. Thaler, and H. X. Zhu, *Phys. Rev. Lett.* **130**, 051901 (2023), 2201.07800.
- [23] C. Andres *et al.*, *Phys. Rev. Lett.* **130**, 262301 (2023), 2209.11236.
- [24] C. Andres, F. Dominguez, J. Holguin, C. Marquet, and I. Moulton, *JHEP* **09**, 088 (2023), 2303.03413.
- [25] C. Andres, F. Dominguez, J. Holguin, C. Marquet, and I. Moulton, *Phys. Rev. D* **110**, L031503 (2024), 2307.15110.
- [26] Z. Yang, Y. He, I. Moulton, and X.-N. Wang, *Phys. Rev. Lett.* **132**, 011901 (2024), 2310.01500.
- [27] C. Andres, F. Dominguez, J. Holguin, C. Marquet, and I. Moulton, *JHEP* **03**, 166 (2025), 2407.07936.
- [28] J. a. Barata, P. Caucal, A. Soto-Ontoso, and R. Szafron, *JHEP* **11**, 060 (2024), 2312.12527.
- [29] J. a. Barata, J. G. Milhano, and A. V. Sadofyev, *Eur. Phys. J. C* **84**, 174 (2024), 2308.01294.
- [30] H. Bossi *et al.*, *JHEP* **12**, 073 (2024), 2407.13818.
- [31] K. Lee and I. Moulton, (2023), 2308.01332.
- [32] K. Lee, I. Moulton, F. Ringer, and W. J. Waalewijn, *JHEP* **01**, 194 (2024), 2308.00028.
- [33] K. Lee, A. Pathak, I. W. Stewart, and Z. Sun, *Phys. Rev. Lett.* **133**, 231902 (2024), 2405.19396.
- [34] H. Chen, P. F. Monni, Z. Xu, and H. X. Zhu, *Phys. Rev. Lett.* **133**, 231901 (2024), 2406.06668.
- [35] J. Holguin *et al.*, (2023), 2311.02157.
- [36] J. Holguin *et al.*, *JHEP* **04**, 072 (2025), 2407.12900.
- [37] M. Xiao, Y. Ye, and X. Zhu, *JHEP* **10**, 088 (2024), 2405.20001.
- [38] W.-J. Xing, S. Cao, G.-Y. Qin, and X.-N. Wang, *Phys. Rev. Lett.* **134**, 052301 (2025), 2409.12843.
- [39] C. Andres, J. Holguin, R. Kunnawalkam Elayavalli, and J. Viinikainen, *Phys. Rev. Lett.* **134**, 082303 (2025), 2409.07514.
- [40] X. Liu, W. Vogelsang, F. Yuan, and H. X. Zhu, *Phys. Rev. Lett.* **134**, 151901 (2025), 2410.16371.
- [41] S. Alipour-fard, A. Budhraj, J. Thaler, and W. J. Waalewijn, (2024), 2410.16368.
- [42] Z.-B. Kang, J. Penttala, and C. Zhang, (2024), 2410.21435.
- [43] J. a. Barata, Z.-B. Kang, X. Mayo López, and J. Penttala, (2024), 2411.11782.
- [44] C. Csáki, S. Ferrante, and A. Ismail, (2024), 2412.02738.
- [45] Y. Fu, B. Müller, and C. Sirimanna, (2024), 2411.04866.
- [46] L. Apolinário *et al.*, (2025), 2502.11406.
- [47] J. a. Barata, I. Moulton, A. V. Sadofyev, and J. a. M. Silva, (2025), 2503.13603.
- [48] H. Chen, H. Ruan, and H. X. Zhu, (2025), 2505.16753.
- [49] K. Lee and I. Stewart, (2025), 2507.11495.
- [50] Y. Guo, F. Yuan, and W. Zhao, (2025), 2507.15820.
- [51] C.-H. Chang *et al.*, (2025), 2507.15923.
- [52] Z.-B. Kang, A. Metz, D. Pitonyak, and C. Zhang, (2025), 2507.17444.
- [53] E. Herrmann, Z.-B. Kang, J. Penttala, and C. Zhang, (2025), 2507.17704.
- [54] A. B. Cuerdo, I. Scimemi, and A. Vladimirov, (2025), 2507.17478.
- [55] I. Moulton and H. X. Zhu, (2025), 2506.09119.
- [56] CMS, A. Hayrapetyan *et al.*, *Phys. Rev. Lett.* **133**, 071903 (2024), 2402.13864.
- [57] ALICE, S. Acharya *et al.*, (2024), 2409.12687.
- [58] STAR, A. Tamis, *PoS HardProbes2023*, 175 (2024), 2309.05761.
- [59] CMS, V. Chekhovsky *et al.*, (2025), 2503.19993.
- [60] ALICE, S. Acharya *et al.*, (2025), 2504.03431.
- [61] A. Nambrath, Energy-energy correlators of inclusive jets from small to large collision systems with the ALICE experiment, talk presented at the Hard Probe 2024, Nagasaki, Japan, September 22-27, 2024, 2024.
- [62] U. A. Wiedemann and U. W. Heinz, *Phys. Rept.* **319**, 145 (1999), nucl-th/9901094.
- [63] T. Sjöstrand, *Comput. Phys. Commun.* **246**, 106910 (2020), 1907.09874.
- [64] T. Kaufmann, A. Mukherjee, and W. Vogelsang, *Phys. Rev. D* **92**, 054015 (2015), 1506.01415, [Erratum: *Phys.Rev.D* **101**, 079901 (2020)].
- [65] Y.-T. Chien, Z.-B. Kang, F. Ringer, I. Vitev, and H. Xing, *JHEP* **05**, 125 (2016), 1512.06851.
- [66] J. Gao, C. Liu, X. Shen, H. Xing, and Y. Zhao, *Phys. Rev. D* **110**, 114019 (2024), 2407.04422.
- [67] D. Neill, I. Scimemi, and W. J. Waalewijn, *JHEP* **04**, 020 (2017), 1612.04817.
- [68] Z.-B. Kang, X. Liu, F. Ringer, and H. Xing, *JHEP* **11**, 068 (2017), 1705.08443.
- [69] Z.-B. Kang, K. Lee, J. Terry, and H. Xing, *Phys. Lett. B* **798**, 134978 (2019), 1906.07187.
- [70] Z. Mi and Z. Wang, One-Point energy correlator inside jets, Preprint, 2025.
- [71] P. Sun, J. Isaacson, C. P. Yuan, and F. Yuan, *Int. J. Mod. Phys. A* **33**, 1841006 (2018), 1406.3073.

Appendix A: “Mixing” Events to Construct the Trivial Correlations

Here we briefly describe the method of event or rather jet mixing used in our work. We use the following procedure:

1. Reconstruct the jets from Pythia and select the jets within certain P_T range, for example $300 \text{ GeV} < P_{T,jet} < 350 \text{ GeV}$.
2. To generate a mixed jet corresponding to a given true jet with n particles, we pick n particles, one each, from n random jets in the same sample, i.e. P_T range, see Fig. 4. Keep track of the energy fraction carried by each particle and the relative angle $\vec{\theta}$ respect to the original jet axis, i.e., $z_i = E_i/E_{J,i}$ and $\vec{\theta}_i$ for particle i from Jet_i .

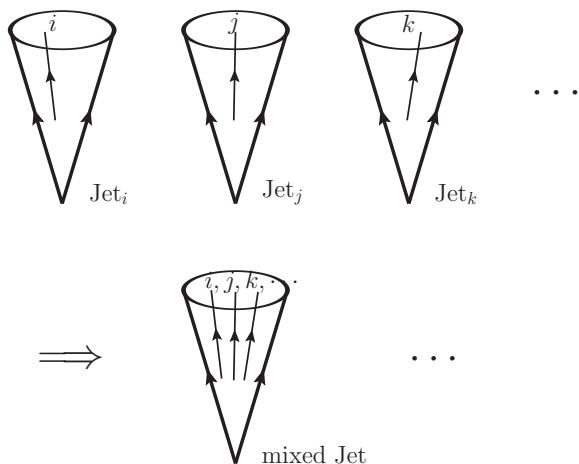


FIG. 4. Construct the mixed jet to evaluate the trivial correlations for the EEC: choosing n particles from randomly chosen jets, such as i, j, k, \dots from $\text{Jet}_i, \text{Jet}_j, \text{Jet}_k, \dots$, respectively, to form a mixed jet. We keep the original energy fraction of each particle and their relative angle $\vec{\theta}$ respect to the original jet axis, e.g., $z_i = E_i/E_{J,i}$ and $\vec{\theta}_i$ for particle i from Jet_i .

3. This procedure will be repeated to have a sufficiently large sample of mixed jets which has the same particle multiplicity distribution within the jets as that of the true jet sample.
4. Calculate the EEC and the single energy flow based on sample of mixed jets by replacing the true jet sample with that of the mixed events in Eqs. (1) and (6), respectively. For example:

$$\begin{aligned} \frac{d\langle E(\theta) \rangle_{\text{mix}}}{d^2\theta} &= \frac{1}{N_{jet}} \sum_{\text{mixed jets } J} \sum_{i \in J} \frac{E_i}{E_{J,i}} \delta^{(2)}(\vec{\theta} - \vec{\theta}_i), \\ \frac{d\langle \text{EEC}(\theta) \rangle_{\text{mix}}}{d^2\theta} &= \frac{1}{N_{jet}} \sum_{\text{mixed jets } J} \sum_{i \neq j \in J} \frac{E_i E_j}{E_{J,i} E_{J,j}} \\ &\quad \times \delta^{(2)}(\vec{\theta} - (\vec{\theta}_i - \vec{\theta}_j)), \end{aligned} \quad (\text{A1})$$

for the single energy flow angular distribution and two particle trivial correlation, respectively.

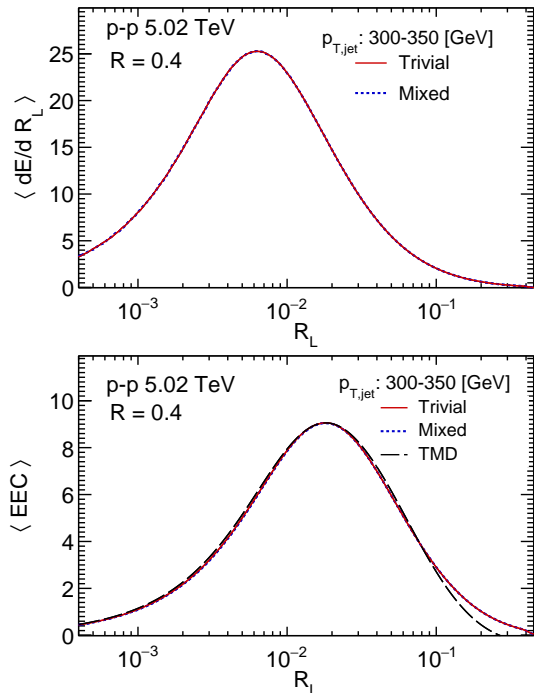


FIG. 5. Mixing jet events to evaluate the trivial correlations: (upper) the angular distribution for single energy flow in the jet for a typical jet energy $P_T = 300\text{-}350\text{GeV}$. (lower) for the trivial correlations in the same P_T range, comparing the mixing jet events simulation (8) with that from integral of single energy flow (7) and the TMD model calculation (B8), see below.

As shown in Fig. 5 (upper panel), the single energy flow from mixed events is identical to the one obtained from the true jet sample, as it should. Furthermore, as shown in the lower panel of Fig. 5 the EEC from mixed events agree with that obtained from the product of the single energy flows, Eq. (7), demonstrating that the EEC from mixed events indeed contains no correlations. As mentioned in the main text, a normalization factor has been included for the jet mixing simulation to ensure the integration results match the value given by Eq. (1).

Appendix B: TMD Description of Particle Distributions in Jet

We start with the single energy flow distribution in a jet, i.e., Eq. (6). As shown in Fig. 1, the particle inside the jet carries the dominant momentum along the jet direction, where the physics can be described by the associated parton fragmentation functions [64–69]. In addition, the momentum projection perpendicular to the jet direction can be regarded as a small transverse momentum, $\vec{P}_{i\perp}^h = z_i E_J \vec{\theta}_i$, where θ_i represents the angular of hadron i with respect to the jet axis, and z_i is

its momentum fraction of the jet energy. A small jet radius implies that the transverse momentum of the hadron $|\vec{P}_{i\perp}^h|$ is much smaller than its longitudinal momentum E_i . Therefore, these distributions can be formulated in terms of the transverse momentum dependent fragmentation functions [4, 67–69]. Applying the TMD fragmentation functions, we have

$$\frac{d\langle E(\theta) \rangle}{d^2\theta} = \mathcal{N}_1 c_1^2 E^2 \sum_h \int dz_h z_h D_{q/g}^h(z_h, P_{h\perp}; \zeta_E), \quad (\text{B1})$$

for Eq. (6), where E represents the jet energy and $D_{q/g}^h(z_h, P_{h\perp})$ with $P_{h\perp} = c_1 z_h E \theta$ denotes the TMD fragmentation function of hadron h within the quark/gluon jet. The factors z_h in Eq. (B1) corresponds to the energy weight in Eq. (6). In the above equation, we introduce a parameter c_1 to represent the average energy fraction that the fragmenting quark/gluon carries respect to the jet energy. We have also introduced a normalization factor \mathcal{N}_1 , which accounts for the contribution from the perturbative matching and has a mild dependence on the jet energy [67–69]. In addition, the TMD fragmentation function will introduce a dependence on the jet energy represented by the Collins parameter $\zeta_E \sim c_2 E$ [4, 68],

$$D_{q/g}^h(z_h, P_{h\perp}; \zeta_E) = \int \frac{d^2 b_T}{(2\pi)^2} e^{i \frac{P_{h\perp} \cdot b_T}{z_h}} D_{q/g}^h(z_h, \mu_b) \times e^{-\frac{S_{q/g}(c_2 E, b_T)}{2}}, \quad (\text{B2})$$

where $S_{q/g}(\zeta_E, b_T)$ is the associated Sudakov form factor (defined below in Eq. (B4)) and $D_{q/g}^h(z_h, \mu_b)$ is the integrated fragmentation function at the scale $\mu_b = 2e^{-\gamma_E}/b_T$ with γ_E the Euler constant. Taking into account the identity $\int dz_h z_h D_{q/g}^h(z_h, \mu) \equiv 1$, we derive the individual energy flow distribution as,

$$\frac{d\langle E(\theta) \rangle}{d^2\theta} = \mathcal{N}_1 c_1^2 E^2 \int \frac{d^2 b_T}{(2\pi)^2} e^{i c_1 E \vec{\theta} \cdot \vec{b}_T} e^{-\frac{S_{q,g}(c_2 E, b_T)}{2}}. \quad (\text{B3})$$

In the above equations, the Sudakov form factors take into account all order soft gluon resummation,

$$S_{q/g}(Q, b) = S_{NP}(b) + \int_{\mu_0^2}^{Q^2} \frac{d\mu^2}{\mu^2} \left[A_{q/g} \ln \frac{Q^2}{\mu^2} + B_{q/g} \right], \quad (\text{B4})$$

where functions A, B can be expanded in terms of α_s : $A(\alpha_s) = \sum_{n=1} \left(\frac{\alpha_s}{\pi}\right)^n A^{(n)}$, $B(\alpha_s) = \sum_{n=1} \left(\frac{\alpha_s}{\pi}\right)^n B^{(n)}$. To illustrate the resummation effects, our numerical calculations take the simple leading terms of $A^{(1)}$ and $B^{(1)}$,

$$A_q^{(1)} = C_F, \quad A_g^{(1)} = C_A, \quad (\text{B5})$$

$$B_q^{(1)} = -\frac{3}{2}C_F, \quad B_g^{(1)} = -2\beta_0. \quad (\text{B6})$$

In addition, we follow Ref. [71] to parameterize the non-perturbative TMD as

$$S_{NP}(b) = \frac{2g_1}{c_1^2} b^2 + g_2 \ln\left(\frac{b}{b_*}\right) \ln \frac{Q}{\mu_0}, \quad (\text{B7})$$

where we have taken the average parton momentum fraction c_1 to modify the TMD fragmentation function parameterization and $b_* = b/\sqrt{1+b^2/b_{\max}^2}$. For the quark EEC, we follow Ref. [71] to set $g_1 = 0.042 \text{ GeV}^2$, $g_2 = 0.84$, $\mu_0 = 1.55 \text{ GeV}$, and $b_{\max} = 1.5 \text{ GeV}^{-1}$. For the gluon counterpart, g_1 and g_2 will be multiplied by a factor C_A/C_F .

Finally, substituting Eqs. (B3) into Eq. (7), we will be able to derive the trivial EEC in terms of the TMD fragmentation functions,

$$\begin{aligned} & \frac{d}{d^2\theta} \langle \text{EEC}(\theta) \rangle_{\text{trivial}} \\ &= \tilde{\mathcal{N}} c_1^2 E^2 \int db b J_0(c_1 E b \theta) e^{-S_{q,g}(c_2 E, b)}, \end{aligned} \quad (\text{B8})$$

where $\tilde{\mathcal{N}} = N_{\text{trivial}} \mathcal{N}_1^2$. Again, this parameter will have a mild energy dependence to account for the perturbative matching to the TMD fragmentation functions in the jet evolution.

In Fig. 5, we include the prediction from the TMD model calculation with the parameter choice of $c_1 = 0.62$, $c_2 = 0.30$ and $\mathcal{N} = 0.65$ for the P_T bin between 300 to 350 GeV with an average jet $P_T = 321 \text{ GeV}$. Clearly, the TMD model calculations capture the main behavior of the trivial correlators at small angles.